Iodotyrosines are biomarkers for preclinical stages of iodine-deficient hypothyroidism in *Dehal1* knockout mice.

Cristian González-Guerrero[1#], Marco Borsò[2#], Pouya Alikhani[1#], Yago Alcaina[1,3], Federico Salas-Lucia[1,4], Xiao-Hui Liao[4], Jorge García-Giménez[1], Andrea Bertolini[2], Diana Martin[3], Adrian Moratilla[3], Roberto Mora[5], Antonio Buño-Soto[5], Ali R. Mani[6], Juan Bernal[7], Alessandro Saba[2], María P. de Miguel[3], Samuel Refetoff[4,8], Riccardo Zucchi[2], José Carlos Moreno[1*]

Affiliations:
[1] Thyroid Molecular Laboratory. Institute for Medical and Molecular Genetics (INGEMM), La Paz University Hospital Research Institute (IdIPAZ). Autonomous University of Madrid (UAM). Spain.
cristian.gonzalez.guerrero@gmail.com, pouya.alikhani2018@gmail.com, yalcaina@gmail.com, jogarcg@gmail.com, josecarlos.moreno@salud.madrid.org

[2] Department of Pathology, Laboratory of Biochemistry. University of Pisa. Italy.
marco.borso@student.unisi.it, a.bertolini2@student.unisi.it, alessandro.saba@unipi.it, riccardo.zucchi@unipi.it

[3] Cell Engineering Laboratory, La Paz Hospital Research Institute. IdiPAZ, Madrid, Spain.
dianamartinlorenzo@gmail.com, amoratillariofrio@gmail.com, mariapdemiguel@gmail.com

[4] Department of Medicine. The University of Chicago, Chicago, IL, USA.
fsalaslucia@uchciago.edu, xliao1@uchicago.edu, srefetof@uchicago.edu

[5] Department of Analytical Chemistry. La Paz University Hospital. Madrid Spain.
roberto.mora@salud.madrid.org, antonio.buno@salud.madrid.org

[6] Division of Medicine, University College London (UCL), London. United Kingdom.
a.r.mani@ucl.ac.uk

[7] Instituto de Investigaciones Biomédicas, Consejo Superior de Investigaciones Científicas (CSIC). Madrid. Spain.
jbernal@iib.uam.es

[8] Department of Pediatrics and Committee on Genetics, The University of Chicago, IL, USA.
srefetof@uchicago.edu

[9] Rare Diseases Networking Biomedical Research Centre (CIBERER). Instituto de Salud Carlos III (ISCIII). Spain.
josecarlos.moreno@salud.madrid.org

# These authors contributed equally to the manuscript.
* Corresponding author:

Dr. José C. Moreno, MD, PhD.
Thyroid Molecular Laboratory.
Institute for Medical and Molecular Genetics (INGEMM).
La Paz University Hospital.
Paseo de La Castellana 264
28046 Madrid. Spain
Phone: (+34) 917277217- ext. 2892
Mobile: (+34) 608312903
Email: josecarlos.moreno@salud.madrid.org

Email-2: j.morenonavarro@gmail.com
ORCID: 0000-0001-5664-5308

ABSTRACT

BACKGROUND. Iodine is required for the synthesis of thyroid hormone (TH), but its natural availability is limited. Dehalogenase1 (Dehal1) recycles iodine from mono- and di-iodotyrosines (MIT, DIT) to sustain TH synthesis when iodine supplies are scarce, but its role in the dynamics of storage and conservation of iodine is unknown.

METHODS. *Dehal1* knockout mice (*Dehal1*KO) were generated by gene-trapping. The timing of expression and distribution was investigated by X-Gal staining and immunofluorescence using recombinant Dehal1-Betagalactosidase protein produced in fetuses and adult mice. Adult *Dehal1*KO and wild-type (*Wt*) animals were fed normal and iodine-deficient diets for 1 month and plasma, urine and tissues were isolated for analyses. TH status was monitored including T_4, T_3, MIT, DIT, and urinary iodine concentration using a novel LC-MS-MS method and the Sandell-Kolthoff (S-K) technique throughout the experimental period.

RESULTS. Dehal1 is highly expressed in the thyroid, is also present in kidneys, liver, and, unexpectedly, the choroid plexus. *In vivo* transcription of *Dehal1* was induced by iodine deficiency only in the thyroid tissue. Under normal iodine intake, *Dehal1*KO mice were euthyroid, but they

showed negative iodine balance due to a continuous loss of iodotyrosines in the urine. Counter-intuitivelythe urinary iodine concentration of *Dehal1KO* mice is two-fold higher than in *Wt* mice, indicating S-K measures both inorganic and organic iodine. Under iodine restriction, *Dehal1*KO mice rapidly develop profound hypothyroidism while *Wt* mice remain euthyroid, suggesting reduced retention of iodine in the thyroids of *Dehal1*KO mice. Urinary and plasma iodotyrosines were continually elevated throughout the life cycles of *Dehal1*KO mice, including the neonatal period, when pups were still euthyroid.

CONCLUSIONS. Plasma and urine iodotyrosine elevation occurs in Dehal1-deficient mice throughout life. Therefore, measurement of iodotyrosines predicts an eventual iodine shortage and development of hypothyroidism in the pre-clinical phase. The prompt establishment of hypothyroidism upon the start of iodine restriction suggests that *Dehal1*KO mice have low iodine reserves in their thyroid glands, pointing to defective capacity for iodine storage.

INTRODUCTION

Iodine deficiency (ID) has severe adverse effects on human health, due to inadequate thyroid hormone (TH) production (1). Nearly two billion individuals in the world are at risk for iodine deficiency, with pregnant women and children being the most vulnerable (1,2). Despite its global prevalence and its dramatic consequences during pregnancy and childhood, early detection of incipient ID in individuals is not currently possible. nternational efforts were implemented to identify human populations with poor iodine intakes using the median urinary iodine concentration (UIC). However, UIC is not useful to diagnose ID individually, since it depends on the recent iodine intake, which is typically variable, and not on iodine reserves. In fact, the need for more efficient markers of ID reflecting individual iodine *status* was recently emphasized (3,4). Such biomarkers must relate to genetic factors modulating the efficiency of iodine handling pathways.

Dehalogenase1 (DEHAL1) also known as iodotyrosine deiodinase (IYD) is a key enzyme for iodine metabolism in the thyroid gland. It removes iodine from mono- and di-iodotyrosines (MIT, DIT), making the former available for recycling and reuse in the thyroid gland to sustain thyroxine (T_4) and triiodothyronine (T_3) synthesis (5,6). Loss-of-function *DEHAL1* mutations were shown to cause severe goitrous hypothyroidism and mental retardation (7). However, the time of onset of such hypothyroidism is unpredictable (7,8), suggesting the influence of environmental conditions in the expression of the disorder. Unfortunately, neonatal screening programs do not detect hypothyroidism of this origin, but the reason is elusive. Therefore, there is a need for further investigation of the role of ioine recycling and the consequences of abnormal iodine conservation in humans throughout life (9).

To this aim, we generated a *Dehal1* knockout (*Dehal1*KO) mouse using gene-trap technology, allowing us to investigate the dynamic relationship between the external iodine supplies and the development of hypothyroidism under controlled iodine intake.

METHODS

Generation of *Dehal1* knockout mice

Mouse embryonic stem cells (ESCs) containing the *Dehal1* knockout allele engineered through gene-trap were obtained from the knockout mouse project (KOMP) repository (10). Essentially, a targeting vector containing the bacterial β-galactosidase (*lacZ*) as reporter gene and Neomycin (*Neo*) as selection gene was inserted between exon 1 and exon 2 of the wild-type *Dehal1* allele (Figure 1A). Therefore, the *Dehal1* promoter and exon 1 are conserved in the recombinant allele, while exons 2 to 6 are excluded from the mRNA which now contains *lacZ*, allowing the characterization of the *Dehal1* expression pattern (Figure 1A). The targeting vector was electroporated into C57BL/6J ES cells and recombinant clones were selected on antibiotic and expanded. ESC clones verified for *Dehal1*[Flox/Wt] were microinjected into blastocysts derived from albino C57BL/6J-Tyr[c-Brd] mice. Chimeric male mice with germline transmission were backcrossed to C57BL/6J mice and the heterozygous mutants were cross-bred to obtain homozygous mutant mice.

Mouse genotyping

Mice were genotyped by touchdown-PCR using DNA extracted from tail. Primer sequences and conditions are available in Supplemental Table 1.

Quantitative RT-PCR

Mouse tissue RNA was isolated according to the manufacturer's protocol (Macherey-Nagel, Düren, Germany). One μg of RNA was reverse transcribed with Transcriptor cDNA Synthesis Kit (Roche Diagnostics, Basel, Switzerland) and quantitative PCR (qPCR) was performed with Sybr Green dye (Quantabio, Beverly, MA, USA) on an ABI Prism 7900HT Fast Real-Time PCR system (Applied Biosystems, ThermoFisher Scientific, Waltham, MA, USA) using the Delta Ct method. *Dehal1* was amplified with specific primers (Sigma-Aldrich, St. Louis, MO, USA) (Supplemental Table 1). Results were normalized with *Gapdh* and expressed relative to controls.

X-Gal staining

Whole-mount or tissue sections from *Dehal1*KO and *Wt* adult and fetal mice were X-Gal stained following published protocols (11).

Immunofluorescence

B-Galactosidase immunofluorescence was performed after antigen-retrieval using sodium citrate buffer at pH=6 and blocked for 1h in PBS/10% goat serum. Sections were incubated overnight at 4°C with primary antibody β-galactosidase (1:300 dilution; ThermoFisher Scientific, Waltham, MA, USA). Specific secondary Alexa-488 antibody (1:200 dilution; Life Technologies, Carlsbad, CA, USA) was used for 1h at room temperature and sections were mounted with an aqueous agent (ProLong Gold, Scientific, Waltham, MA, USA). Nuclei were counterstained with DAPI (Sigma-Aldrich, St. Louis, MO, USA). Images were obtained using an SP5 confocal microscope (Leica Microsystems, Wetzlar, Germany).

Experimental iodine deficiency

Female 5-6 months old *Wt* and *Dehal1*KO mice were fed a low-iodine diet (TD180914; Envigo, Indianapolis, IN, USA) containing 0.05 μgI/g, and separated into three groups receiving 1400 μgI/L,

200 µgI/L or no-iodine in the drinking water, resulting in total estimated iodine intakes of 5.8 (normal, NID), 1.0 (low, LID) and 0.2 µgI (very low, VLID) per animal/day, respectively (12). Urine was collected using hydrophobic sand (Sodispan Research, Madrid, Spain). Mice were anesthetized with 1.5-2% isoflurane (Esteve Laboratories, Barcelona, Spain) inhalation in O2 (0.9L O2/min) and blood was collected by cardiac puncture. Tissues (thyroid, kidney, and liver) were collected on days 0, 12, and 28. Urine and blood from 10-day- old pups, 1-month juveniles, and 3-month adults, fed regular diet (1.4 µgI /day; SAFE diet), were also collected.

Determination of plasma TSH

Plasma TSH levels were measured by radioimmunoassay as described in detail previously (13).

Determination of MIT, DIT, T_3, and T_4 in plasma and/or urine.

Previously published methods (14-17) were modified to allow the simultaneous quantification of MIT, DIT, T_3, and T_4.

Sample preparation: 100 µL of urine/plasma were added with 5.4 pmol $^{13}C_9$-MIT, 4.0 pmol 13C$_9$-DIT, 2.8 pmol $^{13}C_6$-T_3, and 2.4 pmol $^{13}C_6$-T_4, vortex mixed, equilibrated for 30 min at room temperature; 300 µL of cold-acetone were added, and the obtained mixtures were kept at 4°C for 30 min to achieve an optimal sample deproteinization. Then, samples were centrifuged 10 min at 22780 x g and the resulting supernatants were warmed up to 40 °C and dried under a nitrogen stream. The residues were reconstituted with 200 µL of 3.0 N hydrochloric acid in n-butanol, and incubated for 45 min at 60 °C for the formation of the corresponding butyl esters of tyrosines, THs, and their internal standards. After evaporation to dryness, the samples were reconstituted with 500 µL of 0.1 M potassium acetate buffer (pH=4) and loaded onto Agilent (Santa Clara, CA, USA) Bond-Elut Certify 130 mg SPE cartridges, to perform the extraction according to a procedure previously described (15). The eluate was dried once again under nitrogen and the dried residue was reconstituted with 100 µL of acetonitrile/0.1 M hydrochloric acid (50/50 by volume), and 1µL of it was injected into the LC-MS-MS system. Calibration curves ranged from 0.1 to 100.0 ng/mL and were daily prepared by serial dilution in methanol and derivatized by the same procedure used for the samples.

Instrument layout: AB-Sciex (Concord, Ontario, Canada) QTRAP 6500+ triple quadrupole mass spectrometer with ESI source, coupled to an Agilent (Santa Clara, CA, USA) 1290 UHPLC system, fitted with a 110 Å, 2x50 mm, 3µm particle size, Gemini C18 column (Phenomenex, Torrance, CA).

Operative conditions: the chromatographic separation was carried out as previously reported by Cuzzolino et al. (17). Mass spectrometry operated in positive ions selected reaction monitoring (SRM) mode, by using optimized source and compound parameters to achieve the best possible performances. Three transitions were used to monitor each compound and internal standard: the one with the highest signal/noise ratio was used as a quantifier (Q), while the other two as qualifiers (q). They were the following: MIT-But: 363.9 → 261.8 daltons (Da) (Q), 363.9 → 135 Da (q), 363.9 → 291.0 Da (q); 13C9-MIT-But: 373.1 → 270.1 Da (Q), 373.1 → 143.2 Da (q), 373.1 → 300.2 Da (q); DIT-But: 489.9 → 387.9 Da (Q), 489.9 → 260.9 Da (q), 489.9 → 290.0 Da (q); 13C9-DIT-But: 498.8 → 395.8 Da (Q), 498.8 → 268.8 Da (q), 498.8 → 298.9 Da (q); T_3-But: 707.9 → 605.9 Da (Q), 707.9 → 479.1 Da (q), 707.9 → 651.9 Da (q); 13C6-T_3-But: 713.9 → 611.9 Da (Q), 713.9 → 485.1 Da (q),

713.9 → 657.9 Da (q); T_4-But: 833.9 → 731.99 Da (Q), 833.9 → 605.0 Da (q), 833.9 → 777.9 Da (q); 13C6-T_4-But: 839.9 → 737.9 Da (Q), 839.9 → 611.0 Da (q), 839.9 → 783.8 Da (q). Validation of the method is presented in Supplemental Figure 1.

Urinary Iodine Concentration

Mice urine samples were processed by the modified Sandell-Kolthoff method (18) and expressed relative to creatinine concentrations.

Study approval

Animal studies followed the guidelines from the European Animal Research Ethical Committee and were approved by the Animal Research Ethical Committee of the Autonomous University of Madrid, Spain (Proex-13/17).

Statistics

GraphPad Prism software v5 (San Diego, California, USA) was used for statistical analysis. Results were expressed as mean ± SEM. Differences were assessed by a non-parametric Mann-Whitney test for two independent samples and were considered statistically significant when the p-value was <0.05 (*p< 0.05, **p< 0.01, *** p<0.001).

RESULTS

Characterization of *Dehal1*KO mice

The generation of the *Dehal1*KO mouse by gene-trap technology results in a recombinant protein composed of a truncated Dehal1 protein encoded by exon 1, followed by the β-galactosidase enzyme (trDehal1-βG) under the control of the endogenous *Dehal1* promoter (Figure 1A). Chimeric male mice with germline transmission were bred to successfully generate heterozygous and homozygous *Dehal1*KO mice (Figure 1B). The absence of *Wt* Dehal1 RNA and protein was confirmed in thyroids of homozygous *Dehal1*KO mice (Figures 1C-E). Whole-mount X-Gal labelling at low-power magnification showed the presence of the recombinant Dehal1-β-Gal protein in developing thyroids of *KO* mice from embryonic days 13.5 (E13.5) and E15, as well as in postnatal day 120 (P120) adults (Figure 1F a-c). In P120 *KO* mice, the recombinant protein was highly expressed in the thyroid, staining follicular structures, but not parafollicular cells (Figure 1G a-b).

Tissue expression of Dehal1

The activity of the endogenous promoter driving trDehal1-β-Gal expression was investigated in the developing thyroid, kidney and liver, sites of reported iodotyrosine deiodinase activity (19). At E13.5, X-Gal labelling was detected in the pre-follicular stage of the thyroid, in tubular structures of the kidneys, and was not detected in the liver (Figure 2A). Unexpectedly, intense labelling was identified in epithelial cells of the developing choroid plexus (Figure 2A).

In adult *Dehal*1KO mice, thyrocytes were β-Gal immunoreactive (ir)-positive (Figure 2B a). In kidneys, β-Gal ir-positive cells were observed in proximal convoluted tubules (Figure 2B c) showing a cytoplasmic granular pattern. In the liver, this sensitive technique identified ir-positive hepatocytes lining the central vein (Figure 2B e). In the choroid plexus β-Gal ir-positive epithelial cells and neighbor, ependymocytes were also observed lining the ventricular surface (Figure 2B g).

Dehal1 RNA was most abundant in the thyroid, and expressed in kidneys and liver at two- and three-fold lower levels, respectively (Figure 2C), suggesting Dehal1 could have additional roles in mammalians. Therefore, *Dehal1* expression was investigated in response to iodine deficiency in the three tissues from *Wt* mice. LID and VLID triggered 2- and 3.5-fold increase of *Dehal1* mRNA in the thyroid, but not in kidneys or liver (Figure 2C), indicating that the Dehal1 exerts iodine homeostasis through the thyroid gland.

Dehal1KO mice have negative iodine balance and iodotyrosines urinary loss

A novel LC-MS-MS method with high sensitivity and specificity was developed for the concomitant determination of iodotyrosines and iodothyronines (Figure 3A). Adult *Dehal1*KO mice showed normal plasma concentrations of TSH, T_4, and T_3 when fed NID (Figure 3B). However, they showed 10-fold increased plasma MIT and DIT compared to *Wt* mice ($p<0.0001$) (Figure 3B). In urine, MIT and DIT reached a 30-fold increase in *Dehal1*KO *versus Wt* mice ($p<0.0001$) (Figure 3B), indicating that both plasma and urine iodotyrosines are highly discriminative to unveil *Dehal1* defects in rodents. Finally, *Dehal1*KO mice excrete nearly double the amount of iodine in urine, compared to *Wt* mice ($p< 0.001$) (Figure 3B).

Since mice of both genotypes were fed the same amount of iodine, this indicates that a) *Dehal1*KO mice have negative iodine balance through excess iodine excretion caused, at least in part, by the chronic urinary loss of MIT and DIT, and b) the organic iodide contained in iodotyrosines is measured by S-K, while this technique is usually assumed to report only the inorganic (dietary) iodine content of the urine. This finding may have relevant methodological implications for ID studies (Supplemental Figure 2). In summary, under sufficient iodine supply, *Dehal1*KO mice can sustain euthyroidism, although they have a negative iodine balance. This makes *Dehal1*KO mice extremely vulnerable to iodine shortages. Furthermore, this finding indicates that elevated plasma or urinary iodotyrosines are reliable indexes of iodotyrosine deiodinase deficiency, even under conditions of iodine sufficiency.

Iodotyrosines are increased from early life in *Dehal1*KO mice

As MIT and DIT are increased in adult *Dehal1*KO mice, we investigated iodotyrosine concentrations in early postnatal life. Plasma from 10-day-old pups and plasma and urine from juvenile and young adult *Dehal1*KO and *Wt* mice were analyzed. On NID, pups, juveniles, and young adults of both genotypes showed comparable levels of TSH, T_4, and T_3 (Figure 3C). However, only *Dehal1KO* pups, juveniles, and young adults exhibited a marked increase in plasma MIT and DIT (Figure 3C). This iodotyrosine elevation was particularly large at the neonatal stage (>10-fold increased MIT/DIT in *Dehal1KO vs. Wt* pups), while urines from juvenile and young adult *KO* mice showed a five-fold increase compared to *Wt* (Figure 3C). Of note, UIC was elevated in *Dehal1*KO *vs. Wt* mice only when they reached the adult stage (Figure 3C). This could be attributed to functional immaturity of juvenile (and likely neonatal) kidneys, conferring a unique advantage to iodotyrosines to identify the postnatal disease timely.

The findings show that even normal iodine intake significantly increased iodotyrosines, detectable in plasma and urine from 10-day- old *Dehal1*KO pups which is equivalent to birth in humans, potentially allowing an early diagnosis of the disorder.

Iodine shortage rapidly triggers hypothyroidism in *Dehal1*KO mice

To analyze the role of Dehal1 as a function of controlled iodine supplies, adult *Wt* and *Dehal1*KO mice were fed NID, LID and VLID for 28 days. Plasma TSH, T_4 and T_3, plasma and urinary iodotyrosines, and UIC were determined at 0, 12, and 28 days (Figure 4A). On NID and LID, *Wt* and *Dehal1KO* mice showed comparable TSH, T_4, and T_3 levels (Figure 4B). However, *Dehal1*KO mice fed VLID showed marked elevation of TSH and decreased T_4 and T_3, developing profound hypothyroidism by day 28, while *Wt* mice were euthyroid. Hypothyroidism in *Dehal1*KOs developed in a very short time, being already present on day 12. A transient increase of T_3 was detectable at day 12 in *Dehal1KO* mice, likely related to the reported preferential synthesis of T_3 in ID, mediated by D1 deiodination of T_4 (20). After the T_3 peak, a complete failure of TH synthesis occurred in *Dehal1*KO, while *Wt* mice stayed euthyroid (Figure 4B).

Regarding iodotyrosines, *Dehal1*KO mice on NID showed a large elevation of plasma MIT and DIT compared to *Wt* mice while, on LID, iodotyrosine levels declined progressively, but always remained higher than in *Wt* mice (p> 0.005). By contrast, VLID (along with severe hypothyroidism) caused a steep decrease of iodotyrosines in *Dehal1*KO mice so that significant differences between genotypes became no longer detectable at the end of the experiment (Figure 4B).

In urine, iodotyrosines mirrored the changes in plasma (Figure 4C), however, despite a decreasing trend when on iodine restriction, MIT and DIT concentrations remained markedly higher in *Dehal1KO* mice throughout the experiment (p<0.001 at d28) (Figure 4C). Notwithstanding, DIT, which has two iodine atoms, showed a steeper decrease than MIT in *Dehal1*KO mice on VLID, probably reflecting the depletion of iodine reserves. Finally, UIC was significantly higher in Dehal1*KO vs. Wt* mice only on NID and LID diets, with no difference detectable between genotypes on VLID (Figure 4C).

Regarding iodotyrosines, *Dehal1*KO mice on NID showed a large elevation of plasma MIT and DIT compared to *Wt* mice while, on LID, iodotyrosine levels declined progressively, but always remained higher than in *Wt* mice (p> 0.005). By contrast, VLID (along with severe hypothyroidism) caused a steep decrease of iodotyrosines in *Dehal1*KO mice so that significant differences between genotypes became no longer detectable at the end of the experiment (Figure 4B).

In urine, iodotyrosines mirrored the changes in plasma (Figure 4C), however, despite a decreasing trend when on iodine restriction, MIT and DIT concentrations remained markedly higher in *Dehal1KO* mice throughout the experiment (p<0.001 at d28) (Figure 4C). Notwithstanding, DIT, which has two iodine atoms, showed a steeper decrease than MIT in *Dehal1*KO mice on VLID, probably reflecting the depletion of iodine reserves. Finally, UIC was significantly higher in Dehal1*KO vs. Wt* mice only on NID and LID diets, with no difference detectable between genotypes on VLID (Figure 4C).

In summary, the findings indicate a marked sensitivity of *Dehal1*-deficient mice to ID, developing severe hypothyroidism in a very short time.

DISCUSSION

Considering the central role of Dehal1 in iodine metabolism, we investigated the first mammalian model of dehalogenase deficiency under graded iodine supplies.

Our study showed that *Dehal1*KO mice have a negative iodide balance compared to normal mice under conditions of iodine sufficiency due to the large excretion of iodotyrosines in plasma and urine. This abnormality is reflected in the UIC of *Dehal1*KO mice since, contrary to standard thinking, the S-K technique measured both inorganic and organic (iodotyrosines) iodine. In a translational view, this could reduce the efficacy of S-K to detect "low iodine intakes" from urines eventually containing iodotyrosines.

Further, we identified that *Dehal*KO mice on iodine restriction develop profound hypothyroidism in a surprisingly short time compared to normal mice, which remain euthyroid in our experimental design. This indicates that the thyroids of *Dehal*KO mice do not contain enough iodine reserves to compensate (even very short) periods of iodine shortage, suggesting a relevant role of Dehal1 in iodine storage during iodine sufficiency. Thus, Dehal1 activity revealed necessary not only in scenarios of iodine resriction to "salvage iodine" for TH synthesis but as an enzyme governing the efficient building-up of iodine reserves in the thyroid gland. Further research on the mechanisms how Dehal1 influences iodine storage in the thyroid is warranted.

Our findings may have important clinical implications. In humans, the determination of MIT and DIT may be useful for the diagnosis of DEHAL1 defects when hypothyroidism is present but, most importantly, before hypothyroidism is established. This could be particularly relevant for neonates since, as shown here for mice, affected babies may not show hypothyroidism at birth, but iodotyrosines could be invariably elevated. This would allow detection of the risk for hypothyroidism when the brain is actively developing, thus helping the prevention of mental retardation (7,8). Our experimental model needs to be extended to precisely define the dynamics of iodine conservation in chronic ID or in circumstances of increased iodine demands, such as pregnancy, where our model can be instrumental to investigate the consequences for the progeny (21).

Finally, the expression of Dehal1 in extra-thyroidal tissues is intriguing, especially in the choroid plexus. Further to its capacity for deiodination, Dehal1 can debrominate and dechlorinate tyrosines (22,23). Recently, essential functions for bromide and chloride were unveiled in the brain (24,25), encouraging the investigation of whether Dehal1 could participate in cell homeostasis of other halogens in specific tissues.

In conclusion, Dehal1 is a key factor for iodine metabolism in the thyroid gland. In periods of iodine deficiency, it allows the reuse of iodine from iodotyrosines for hormone synthesis, but in iodine sufficiency, it contributes to optimal iodine storage in the thyroid gland. The model of dehalogenase deficiency presented here supports the proposed paradigm that genetic factors mediate the relation between *iodine nutrition* and *iodine status* (reserves). From a translational perspective, elevated

iodotyrosines are biomarkers for the risk and vulnerability to iodine-deficient hypothyroidism in asymptomatic individuals with defective iodine-recycling that now await validation in the clinical arena.

AUTHORSHIP CONTRIBUTION

Cristian González-Guerrero [#], Marco Borsò [#] and Pouya Alikhani [#] designed and conducted experiments, analysed data, and contributed to the generation of Figures and the draft of the manuscript. Yago Alcaina, Federico Salas Lucia, Xiao-Hui Liao, Jorge García-Giménez, Andrea Bertolini, Diana Martín, Adrian Moratilla, Roberto Mora and Ali R. Mani contributed to the methodology. Antonio Buño-Soto, Ali R. Mani, Alessandro Saba and María P. de Miguel validated data and supervised methodology. Ali R. Mani, María P. de Miguel, Alessandro Saba, Juan Bernal, and Samuel Refetoff provided intellectual input into the design of the study and reviewed and edited the manuscript. José Carlos Moreno and Riccardo Zucchi conceived the project, wrote the manuscript and acquired funding and resources for the study.

[#] The co-first authors contributed to the vast majority of the experimental design and execution at separate and collaborating Institutions through time. To assign the order, the relevance and time invested to complete their respective contributions were considered.

AUTHOR DISCLOSURE

All authors have nothing to disclose.

REFERENCES

1. Zimmermann MB, Boelaert K. Iodine deficiency and thyroid disorders. Lancet Diabetes Endocrinol. 2015; 3(4): 286-95; doi: 10.1016/S2213-8587(14)70225-6
2. Zimmermann MB. The Importance of adequate iodine during pregnancy and infancy. World Rev Nutr Diet. 2016;115: 118-24; doi: 10.1159/000442078

3. Pearce EN, Kathleen L, Caldwell KL. Urinary iodine, thyroid function and thyroglobulin as biomarkers of iodine status. Am J Clin Nutr 2016;104 Suppl 3(Suppl 3): 898S-901S; doi: 10.3945/ajcn.115.110395

4. Rohner F, Zimmermann M, Jooste P, et al. Biomarkers of nutrition for development-iodine review. J Nutr 2014; 144(8): 1322S-1342S; doi: 10.3945/jn.113.181974

5. Moreno JC, Visser TJ. Genetics and phenomics of hypothyroidism and goiter due to iodotyrosine deiodinase (DEHAL1) gene mutations. Mol Cell Endocrinol. 2010; 322(1-2): 91-8; doi: 10.1016/j.mce.2010.03.010

6. Kopp PA. Reduce, recycle, reuse - iodotyrosine deiodinase in thyroid iodide metabolism. N Engl J Med. 2008; 358(17): 1856-9; doi: 10.1056/NEJMe0802188.

7. Moreno JC, Klootwijk W, van Toor H, et al. Mutations in the iodotyrosine deiodinase gene and hypothyroidism. N Engl J Med. 2008; 358(17):1811-8; doi: 10.1056/NEJMoa0706819

8. Iglesias A García-Nimo L, Cocho de Juan JA, Moreno JC. Towards the pre-clinical diagnosis of hypothyroidism caused by iodotyrosine deiodinase (DEHAL1) defects. Best Pract Res Clin Endocrinol Metab 2014; 28(2): 151-9; doi: 10.1016/j.beem.2013.10.009

9. Hlucny K, Alexander BM, Gerow K, et al. Reflection of dietary iodine in the 24 h urinary iodine concentration, serum iodine and thyroglobulin as biomarkers of iodine status: A pilot study. Nutrients. 2021; 13(8): 2520; doi: 10.3390/nu13082520

10. Hansen GM, Markesich DC, Burnett MB, et al. Large-scale gene trapping in C57BL/6N mouse embryonic stem cells. Genome Res. 2008; 18(10): 1670-9; doi: 10.1101/gr.078352.108

11. Gierut JJ, Jacks TE, Haigis KM. Whole-mount X-Gal staining of mouse tissues. Cold Spring Harb Protoc. 2014; 2014(4): 417-9; doi: 10.1101/pdb.prot073452

12. Bianco AC, Anderson G, Forrest D et al. American Thyroid Association Guide to investigate thyroid hormone economy and action in rodent and cell models. Thyroid. 2014; 24(1): 88-168; doi: 10.1089/thy.2013.0109

13. Pohlenz J, Maqueem A, Cua K, et al. Improved radioimmunoassay for measurement of mouse thyrotropin in serum: strain differences in thyrotropin concentration and thyrotroph sensitivity to thyroid hormone. Thyroid. 1999; 9(12): 1265-71; doi: 10.1089/thy.1999.9.1265

14. Borsò M, Agretti P, Zucchi R, et al. Mass spectrometry in the diagnosis of thyroid disease and in the study of thyroid hormone metabolism. Mass Spectrom Rev. 2020; 41(3):443-468; doi: 10.1002/mas.21673

15. Saba A, Chiellini G, Frascarelli S, et al. Tissue distribution and cardiac metabolism of 3-iodothyronamine. Endocrinology 2010; 151(10): 5063-73; doi: 10.1210/en.2010-0491

16. Saba A, Donzelli R, Colligiani D, et al. Quantification of thyroxine and 3,5,3'-triiodo-thyronine in human and animal hearts by a novel liquid chromatography-tandem mass spectrometry method. Horm Metab Res 2014; 46(9): 628-34; doi: 10.1210/en.2010-0491

17. Guzzolino E, Milella MS, Forini F, et al. Thyroid disrupting effects of low-dose dibenzothiophene and cadmium in single or concurrent exposure: new evidence from a

translational zebrafish model. Sci Total Environ. 2021; 769: 144703. doi: 10.1016/j.scitotenv.2020.144703

18. Benotti J, Benotti N. Protein-bound iodine, total iodine, and butanol-extractable iodine by automation. Clin Chem 1963; 12: 408–416; PMID: 14060192

19. Mathi AA, Gaupale TC, Dupuy C, et al. Expression pattern of iodotyrosine dehalogenase 1 (DEHAL1) during chick ontogeny. Int J Dev Biol 2010; 54(10): 1503-8; doi: 10.1387/ijdb.092932am

20. Pedraza PE, Obregon MJ, Escobar-Morreale HF, et al. Mechanisms of adaptation to iodine deficiency in rats: thyroid status is tissue specific. Endocrinology 2006; 147(5): 2098-108; doi: 10.1210/en.2005-1325

21. Berbel P, Navarro D, Román GC. An evo-devo approach to thyroid hormones in cerebral and cerebellar cortical development: etiological implications for autism. Front Endocrinol (Lausanne). 2014 Sep 9; 5: 146; doi: 10.3389/fendo.2014.00146

22. McTamney PM, Rokita SE. A mammalian reductive deiodinase has broad power to dehalogenate chlorinated and brominated substrates. J Am Chem Soc. 2009; 131(40): 14212-3; doi: 10.1021/ja906642n

23. Mani AR, Moreno JC, Visser TJ, et al. The metabolism and de-bromination of bromotyrosine in vivo. Free Radic Biol Med. 2016; 90: 243-251; doi: 10.1016/j.freeradbiomed.2015.11.030

24. McCall AS, Cummings CF, Bhave G, et al. Bromine is an essential trace element for assembly of collagen IV scaffolds in tissue development and architecture. Cell 2014; 157(6): 1380-1392; doi: 10.1016/j.cell.2014.05.009

25. Fukuda A. Chloride homeodynamics underlying modal shifts in cellular and network oscillations. Neurosci Res. 2020; 156: 14-23; doi: 10.1016/j.neures.2020.02.010

FIGURE LEGENDS

Figure 1: Dehal1KO mouse generation and characterization. A, Generation of *Dehal1* knockout (*Dehal1*KO) mouse using a targeting vector containing *lacZ* as reporter gene and *Neo* as selection gene, introduced by homologous recombination between exons 1 and 2 of *Dehal1* wild type (*Wt*) allele. The vector also contains the mouse En2 splice acceptor as a trapping cassette for *lacZ*, predicting the generation of a *Dehal1* null allele through splicing between *Dehal1* exon 1 donor sequences and the *lacZ* trapping cassette. An SV40 polyadenylation (PA) sequence cassette ensures the stability of the recombinant mRNA. **B,** PCR genotyping from genomic DNA and allele-specific primers showing amplification of 650-bp and 550-bp bands on agarose electrophoresis of *Wt* homozygous (*Wt*), *Dehal1*KO heterozygous (HT) and homozygous (HO) mice, respectively (*Dehal1*: primers were specific for *Wt*-allele amplification; *Neo*: primers were specific for the KO-allele. **C-D,** *Dehal1* mRNA amplification from *Wt* and *Dehal1*KO mice by RT-PCR **(C)** and quantitative PCR (6-9 thyroids per group) **(D). E,** Western blotting using Dehal1-specific polyclonal antibodies. **F,** Whole-mount macroscopic images showing X-Gal blue staining of thyroid gland lobules in *Dehal1*KO embryos at days 13.5 (E13.5) **(a,** faint), 15.5 (E15.5) **(b,** intense), and in adult *Wt* **(c). G,** Microscopic

images of thyroid gland slices from *Dehal1*KO mice showing X-Gal blue staining of the thyrocytes, composing the tissue specific-follicular architecture **(a)** while follicles from *Wt* mice remain unstained **(b) (**Microscopic images at 400x amplification. Scale bar 50 µm).

Figure 2. Extra-thyroidal expression of Dehal1 in embryos and adult mice. A, X-Gal staining of thyroidal and non-thyroidal tissue slices at embryonal stage (E13.5) of *Dehal*1KO embryos (expressing the recombinant B-galactosidase under the natural *Dehal1* promoter) is detectable in the thyroid gland **(a)**, kidney **(b)** and brain choroid plexus **(d)** (arrows) while undetectable in the liver **(c)** (scale bar 50 µm). **B,** Immunofluorescence of B-Galactosidase (green) and DAPI (blue) in thyroid, kidney, liver and choroid plexus from adult *Dehal1*KO and *Wt* mice. **(a-b)** In the thyroid, confocal micrographs show positive green staining (arrowheads) in the follicular cells from *Dehal1*KO **(a)** while absent in *Wt* mice **(b)**. **(c-d)** In the kidney, Dehal1 is expressed in the convoluted tubular cells of the cortex but is absent in the glomeruli. **(e-f)** In the liver, Dehal1 is expressed exclusively in the hepatocytes surrounding the central vein (CV). **(g-h)** In the choroid plexus, green staining is present in all ependymal cells **(g)** but not in *Wt* ependymocytes **(g)** (scale bars 50µm, except for kidney 25µm. Composite images are defined as merge). **C,** Comparative expression levels of *Dehal1* mRNA in adult thyroid, kidney, and liver tissues and responsiveness to incremental ID (normal, low and very low iodine diets (NID, LID, VLID; 4-6 animals per group), respectively. Results are in mean±SEM (* $p<0,05$;** $p<0,01$; *** $p<0,005$).

Figure 3. Hormonal and biochemical characterization of Wt and Dehal1KO mice. A,
Representative LC/MS-MS chromatogram of four analytes (MIT, DIT, T3, T4) with their isotope-labeled internal standards (IS1-4). For each compound, three transitions were monitored, and based on the height of the signal-to-noise (S/N) ratio, one transition was used as a quantifier (Q) while the other two as qualifiers (q). **B,** Plasma (pl) thyrotropin (TSH), total thyroxine (T4), total triiodothyronine (T3), mono-iodotyrosine (MIT) and di-iodotyrosine (DIT) and urinary (u) concentrations of MIT, DIT and iodine (UIC) were determined in adult Wt and Dehal1KO mice using specific radioimmunoassay (TSH; 10 samples/group)   LC/MS-MS (iodothyronines and iodotyrosines; 23 samples/group) and the Sandell-Kolthoff reaction (UIC; 16-17 samples/group). **C,** Same parameters were investigated in 10-day- old pups and 1-month old juveniles (6-9 samples/group) as compared to adult mice (23 per group), excepting for urinary determinations in pups, due to restrictions in sample collection. Scatter plots of blue circles and red triangles represent values from Wt and Dehal1KO mice, respectively. Results are in mean±SEM (* $p<0,05$;** $p<0,01$; *** $p<0,005$).

Figure 4. Model of incremental iodine deficiency and biochemical characterization of plasma and urine in wild type (*Wt*) and *Dehal1*KO mice. A, Experimental design. Adult mice of both genotypes were fed with diets containing normal (NID, 5.8 µg/day), low (LID, 1 µg/day), and very low (VLID, 0.2 µg/day) iodine content for 28 days. Plasma and urine were collected at baseline,12

days and 28 days, and thyroid tissue at 28 days. **B,** Biochemical characterization of mouse plasma (*p*) in the model, including TSH (by radioimmunoassay) and T$_4$, T$_3$, mono-iodotyrosine (MIT), and di-iodotyrosine (MIT) (by LC/MS-MS). **C,** Biochemical characterization of mouse urine (*u*) in the model, including MIT and DIT (using LC/MS-MS), and urine iodine concentration (UIC) using the spectrophotometric Sandell-Kolthoff method. Grouped scatter plots in blue squares and lines represent data from *Wt* mice while data from *Dehal1*KO mice are represented in red circles and lines (Day 0: 20-22 samples per genotype, days 12 and 28: 7-8 samples per group). Results are in mean±SEM (* p<0,05 vs. *Wt*; ** p<0,01 vs *Wt*; *** p<0,001 vs *Wt*).
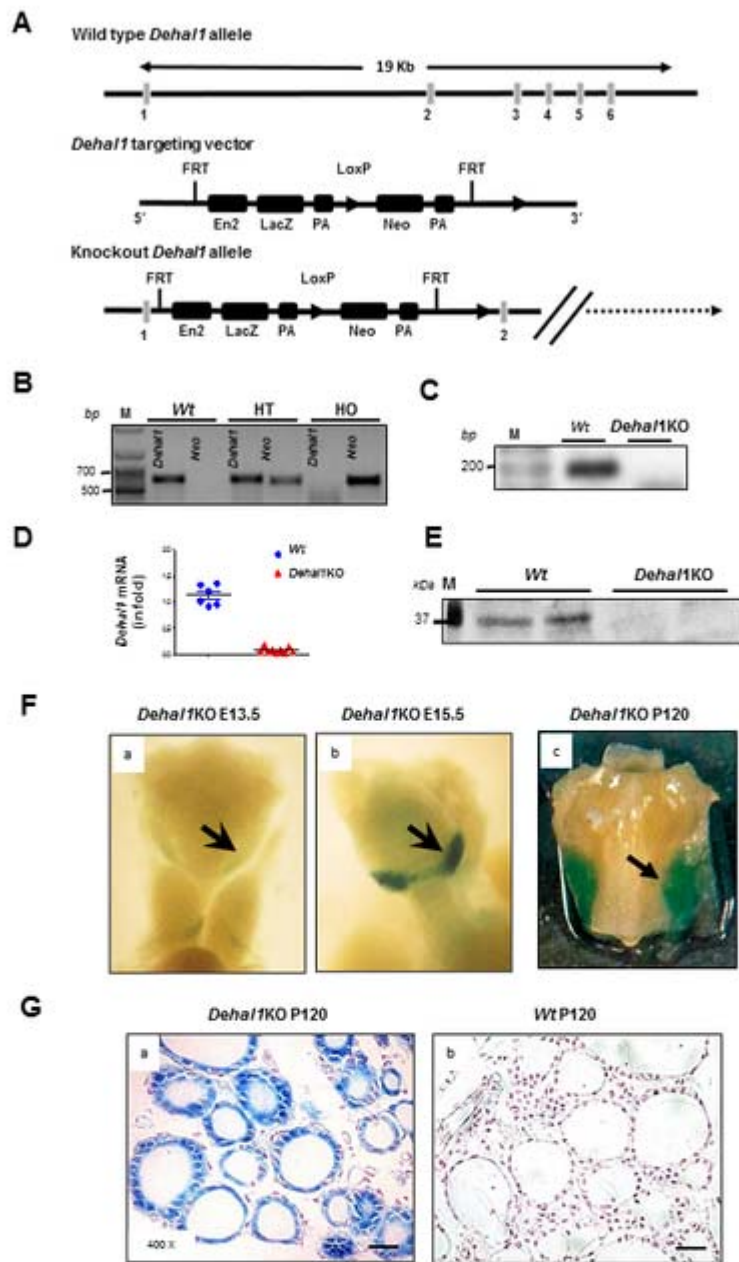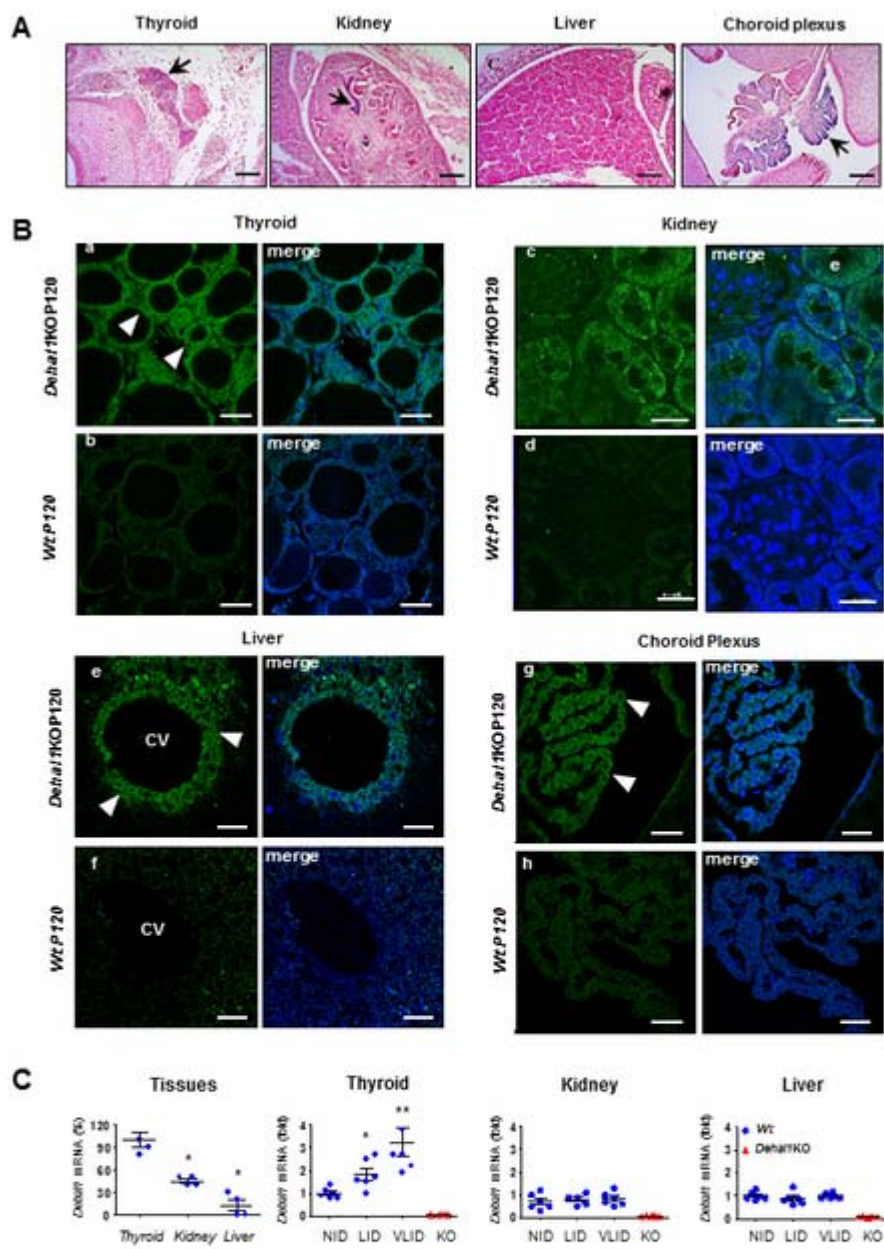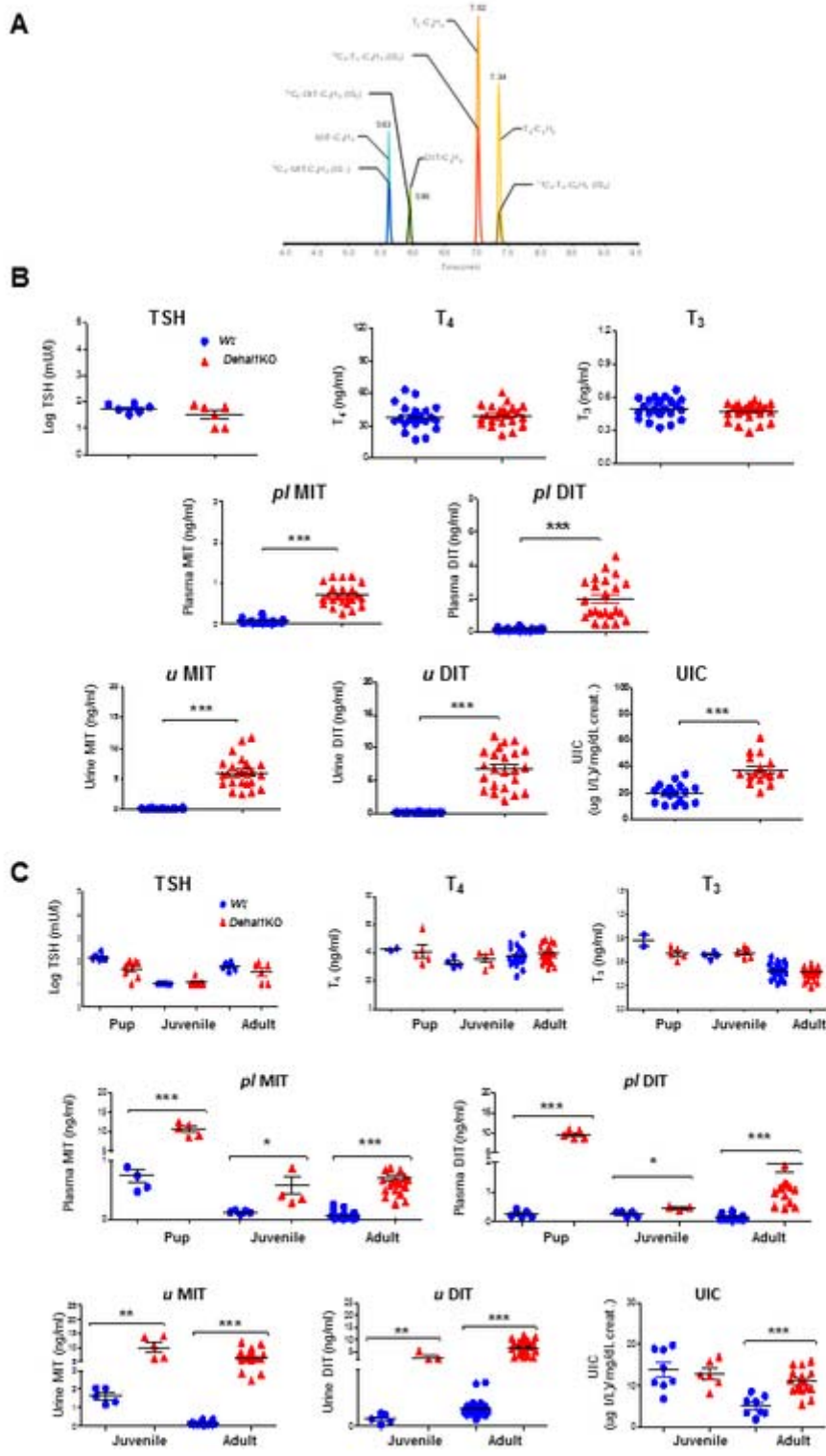
A

Wild type *Dehal1* allele

Dehal1 targeting vector

Dehal1 allele

Knockout *Dehal1* allele

B

C

D

E

F

*Dehal1*KO E13.5   *Dehal1*KO E15.5   *Dehal1*KO P120

G

*Dehal1*KO P120   *Wt* P120

Figure 1

Figure 2

Figure 3
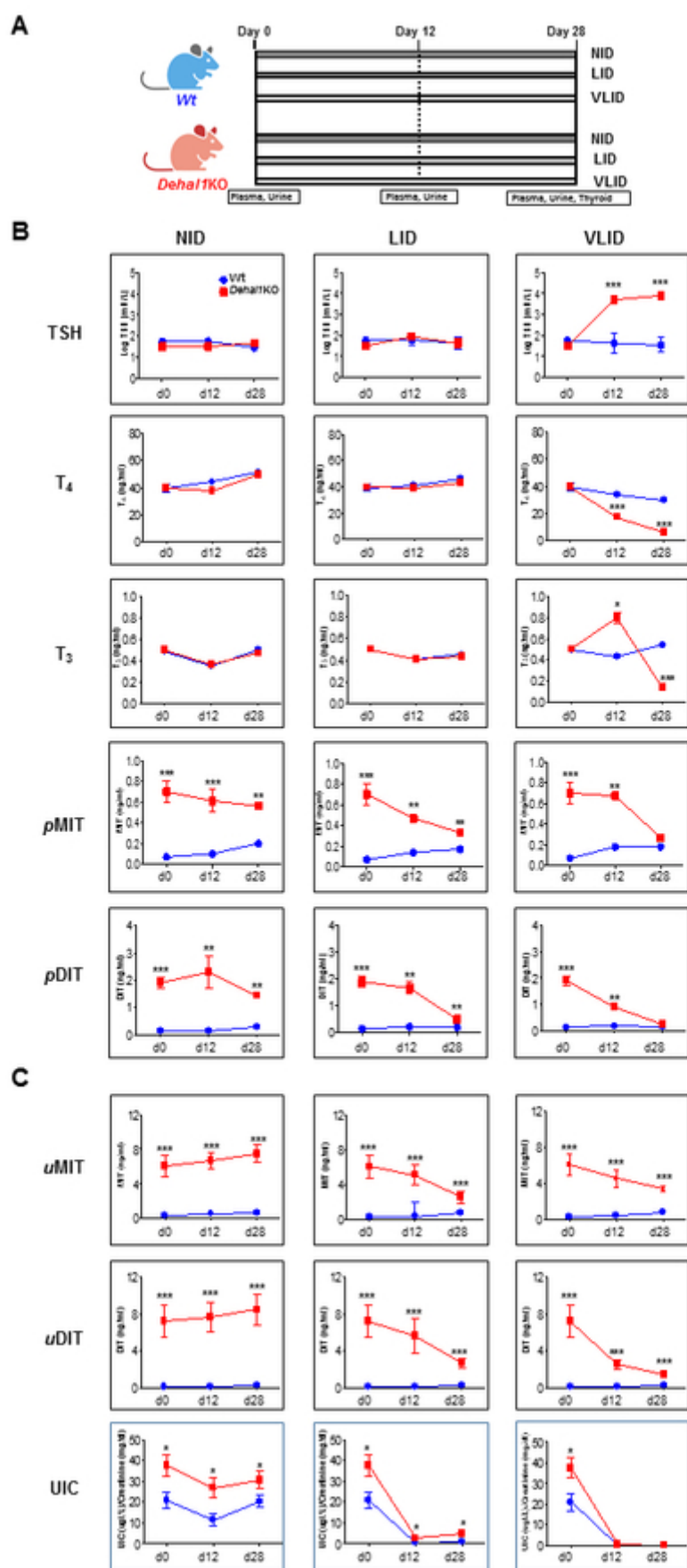
Figure 4

Supplemental Figures and Tables:

A

Analyte	Retention time (min)	Slope (m)	Intercept (q)	Correlation (r^2)
MIT-C_4H_9	5.63 ± 0.01	0.0521 ± 0.0129	0.0050 ± 0.0018	0.9991 ± 0.0006
DIT-C_4H_9	5.96 ± 0.01	0.1388 ± 0.0252	0.0089 ± 0.0048	0.9991 ± 0.0006
T_3-C_4H_9	7.02 ± 0.01	0.0342 ± 0.0190	0.0023 ± 0.0021	0.9989 ± 0.0009
T_4-C_4H_9	7.34 ± 0.01	0.0245 ± 0.0020	-0.0001 ± 0.0013	0.9988 ± 0.0006

B

Analyte	LOD		LOQ		Accuracy (%)		Recovery		Matrix Effect	
	ng/mL	nM	ng/mL	nM	Plasma	Urine	Plasma	Urine	Plasma	Urine
MIT-C_4H_9	0.05	0.14	0.10	0.28	103.6	114.3	84.4	84.6	78.9	105.0
DIT-C_4H_9	0.02	0.04	0.10	0.20	95.8	107.4	94.1	87.2	112.2	107.3
T_3-C_4H_9	0.01	0.01	0.02	0.03	97.9	NA	76.2	NA	99.6	NA
T_4-C_4H_9	0.01	0.02	0.05	0.06	100.2	NA	63.8	NA	81.0	NA

Suppl. Figure 1

Suppl. Figure 1. Validation of the LC/MS-MS method for determination of iodotyrosines and iodothyronines. A, Retention time stability and linearity were evaluated within the calibration curve range. Data are expressed as Mean±SD. B, Standard quality control variables (1). Sensitivity was assessed by evaluating limits of detection (LOD) and limits of quantification (LOQ) of the analytes, which corresponded to the concentrations providing an S/N ratio close to 3 and 10, respectively, measured with a specific tool of the instrument control and data processing software (ABSciex Analyst® 1.7.2). Accuracy (%) was measured on plasma and urine samples spiked with 3 different concentration levels of analytes (C1, 2.5ng/mL, C2 10 ng/mL, C3 50 ng/mL), and the spiked concentration was determined by subtracting the endogenous concentration, C0, to C1, C2, C3. Accuracy (%) was calculated by the formula [(measured concentration/nominal concentration spiked) x 100]. Recovery was evaluated by comparing the peak areas of the internal standards added before and after the extraction procedure. It was expressed as % and calculated by the formula [(peak area of IS added before the extraction/peak area of IS added after the extraction) x 100]. The estimation of matrix effect (%) was evaluated by comparing the peak area of the internal standard added after the extraction in water (A) and matrix (B) and calculated by the formula [(B/A) x 100]. Remarkably, MIT and DIT limits were lower than reported in a previously published method (2).

References:

1. Matuszewski BK, Constanzer ML, Chavez-Eng CM. Strategies for the assessment of matrix effect in quantitative bioanalytical methods based on HPLC-MS/MS. Anal Chem. 2003;75(13):3019-30; doi: 10.1021/ac020361s.

2 Afink G, Kulik W, Overmars H, et al. Molecular characterization of iodotyrosine dehalogenase deficiency in patients with hypothyroidism J Clin Endocrinol Metab. 2008;93(12):4894-901; doi: 10.1210/jc.2008-0865.
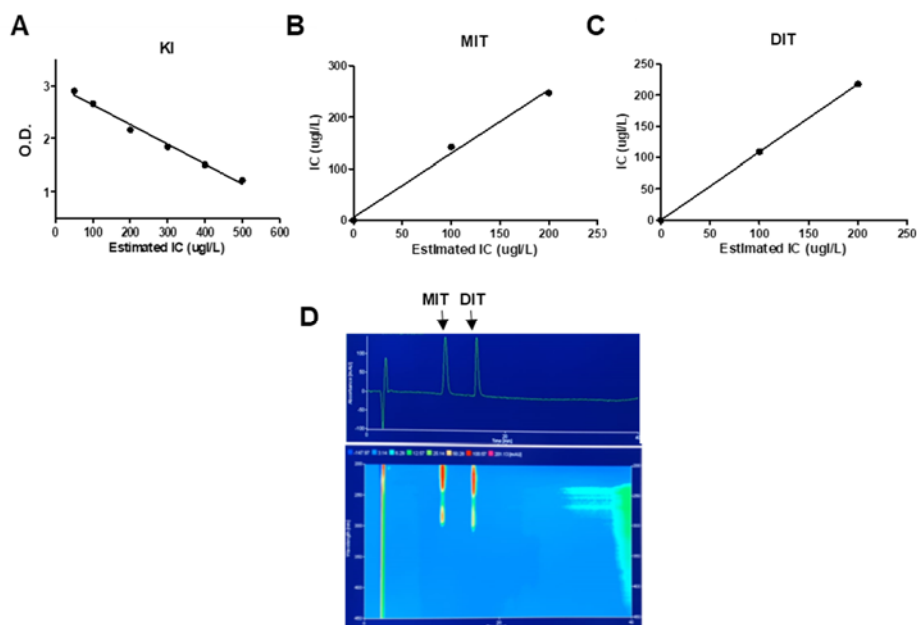
Suppl. Figure 2

Suppl. Figure 2. Iodine Concentration (IC) by Sandell-kothoff (S-K) reaction and the contribution and integrity of iodotyrosines in the performance of the method. A, Stardard curve showing inverse linear correlation between optical density (O.D.) and known molar concentrations of iodide added as Potasium Iodide (KI) to an aquous matrix. B-C, Correlation between IC, assayed by S-K and two different concentrations of iodotyrosines (100 and 200 ug/L) diluted in water, considering the contribution of iodine to their respective molecular weights (MW) (MW of Iodide: 126,9; MW of KI: 166 (76% I); MW of MIT: 307,8 (41% I) and MW of DIT: 432,98 (59% I). The S-K method determines linearly the iodine content of both iodotyrosines, diluted in water. D, Chromatogram showing intact MIT and DIT following incubation with ammonium persulfate and boiling (top) and UV spectrum of the peaks identified on the basis of retention time (bottom).

Supplementary Text

The results suggest that iodine contained in iodotyrosines is measured by the Sandell-Kolthoff (S-K) method, and that iodotyrosines remain intact after the classical digestion by ammonium persulphate and boiling, used in the technique. This indicates that UIC by S-K quantifies both inorganic and organic iodine (from MIT and DIT). Indeed, two decades ago, it was reported that S-K was capable to quantify iodine contained on the digested thyroglobulin (1)

UIC by S-K is assumed to reflect 90% of the iodine intake during the previous 24-48 h that was not taken up by the thyroid (and other organs expressing NIS), thus indicating the recent iodine intake. In virtue of this, S-K has been extensively used to estimate the iodine nutrition in populations. However, if organified iodine species like MIT and DIT are accounted for in S-K, the method might not only reflect iodine intake, but also the (individual) handling of iodine and metabolism at the thyroid gland.

In case iodotyrosines reach relevant concentrations in the urine (indicating variable iodine recycling defects) the contribution of MIT and DIT to total UIC should be considered to evaluate the "iodine intake": iodotyrosines in urine may potentially overestimate the real "iodine intake" of individuals with suboptimal iodide-recycling, since the organic iodine would unadvertedly increase total UIC. This is counter-intuitive from the clinical standpoint.

Strikingly, UIC determined by ICP-MS has been reported to be significantly lower than UIC by S-K (2,3). Such difference was attributed to "higher specificity" of ICP-MS (3), but iodotyrosines were not measured concomitantly. We suggest that iodotyrosines in the urine should be determined in parallel with UIC to clarify inorganic (reflecting intake) *versus* organic (reflecting metabolism) fractions of UIC.

References:

1. Baudry N, Mallet B, Lejeune PJ, et al. A micromethod for quantitative determination of iodoamino acids in thyroglobulin. J Endocrinol. 1997; 153(1): 99-104; doi: 10.1677/joe.0.1530099.
2. Caldwell KL, Maxwell CB, Makhmudov A, et al. Use of inductively coupled plasma mass spectrometry to measure urinary iodine in NHANES 2000: comparison with previous method. Clin Chem. 2003; 49(6 Pt 1): 1019-21; doi:10.1373/49.6.1019.
3. Macours P, Aubry JC, Hauquier B, et al. Determination of urinary iodine by inductively coupled plasma mass spectrometry. J Trace Elem Med Biol 2008; 22(2): 162-5; doi: 10.1016/j.jtemb.2008.02.003.

Gene	Forward primers	Reverse primers
Genomic amplification		
Mouse		
CSDDehal1-F	TTCCTGGGCCAAGCATATTCAAACC	-
CSD-Neo-F	GGGATCTCATGCTGGAGTTCTTCG	-
CSDDehal1-R		AGAAGGGCAGACAGAGAAAGAGACG
cDNA amplification		
Mouse		
Dehal1 (ex: 1-2)	CGACAGGAACCTAGAGAAAA	CTCATTTCCTGTTCTGGGTA
Gapdh	ACATCAAGAAGGTGGTGAAG	TGTAGCCGTATTCATTGTCA

Suppl. Table 1

Supplementary Table 1. Primer sequences used for genotyping mice by touchdown-PCR and for expression of *Dehal1* in thyroid, kidney and liver from mouse tissues.

The touchdown PCR protocol is as follow: *Dehal1*-exon1 forward primer was used in combination with *Dehal1*-specific reverse or Neo-specific reverse primers (Sigma-Aldrich) to respectively amplify *Wt* and *Dehal1*KO alleles. Conditions for touchdown PCR were: 5 min pre-denaturalization at 94ºC, 10 cycles of 15-sec denaturalization at 94ºC, 30-sec annealing at 65ºC but decreasing 1ºC per cycle, and 40-sec extension at 72ºC, followed by 30 cycles using 55ºC as constant annealing temperature, and 5 min extension at 72 ºC.